Fabrication of HARM Structures by Deep-X-ray Lithography Using Graphite Mask Technology

P. Coane*, R. Giasolli*, S. Ledger*, K. Lian, Z. Ling**, J. Göttert*****

**Institute for Micromanufacturing, Louisiana Tech University, P.O. Box 10137, Ruston, LA 71272*
***Center for Advanced Microstructures and Devices, 6980 Jefferson Hwy., Baton Rouge, LA 70806*
****Forschungszentrum Karlsruhe, Project ANKA Team (PEA), P.O. Box 3640, D-76021 Karlsruhe, Germany*

Abstract

The cost-effective fabrication process for high-aspect-ratio microstructures using x-rays depends largely on the availability and quality of x-ray masks. The fabrication of x-ray masks using commercially available graphite sheet stock, as mask membrane is one approach that is designed to reduce cost and turn-around time. Rigid graphite offers unique properties, such as moderate x-ray transmission, fairly low cost, electrical conductivity, and the ability to be used with either subtractive or additive processes [1,2].

This paper will demonstrate the potential of a cost-effective, rapid prototyping of high-aspect-ratio microstructures (HARMs) using graphite masks. The graphite wafer accommodates both the intermediate mask and the working mask. In order to allow a direct comparison of the graphite mask quality with other x-ray masks, the primary pattern was derived from a Ti x-ray mask using soft x-ray lithography (XRL).

1. Introduction

For x-ray based micromachining, applying deep or ultra-deep x-ray lithography (DXRL and UDXRL, respectively) mask fabrication is a critical requirement as it determines costs as well as turn-around time. For many applications the rapid fabrication of prototype structures is important in order to evaluate advantages or improve the design.

It is essential to increase the acceptance of x-ray technology, especially for users from industry. Key issues such as easy accessibility to an exposure station at a synchrotron source, the efficient fabrication of x-ray masks, and process parameter determination for exposures of microstructures with varying heights on a routine basis must be provided. The worldwide effort to enhance the commercial infrastructure is readily apparent from the content of the presentations at the HARMST'99 conference [3].

One contribution to the effort is presented in this paper and refers to x-ray masks. Requirements for x-ray masks in MEMS applications are less critical compared with VLSI applications [4]. Nevertheless, the wide range of height requirements from a few tens of micrometers up to several millimeters has resulted in a variety of mask architectures. In the past, different processes and materials have been used. Except for beryllium, all of these concepts utilize thin film membranes acting as a transparent mask support that requires considerable processing which adds to the cost. The absorber pattern is typically formed from electroplated Au.

For example, in DXRL microstructures of up to 1 millimeter are produced using high-energy photons over a range from 5 keV to 15 keV. Here, a typical x-ray mask consists of a fragile 2-µm-thick silicon or titanium membrane and a gold absorber thickness varying from 5 µm to 15 µm [5,6]. For the fabrication of even higher microstructures in UDXRL, photons with energies up to 40 keV are used. In this case, relatively thick beryllium (300 - 600 µm) [7] and silicon substrates (50 - 400 µm) [8] are acceptable as mask membranes. The required contrast is assured by using a gold absorber with thickness up to 50 µm. To conclude, the fabrication processes are not standardized and typical turn-around times range from 1-2 weeks up to 3 months.

The best candidate for a mask membrane suitable for DXRL and UDXRL is beryllium. It offers the lowest x-ray absorption, good mechanical stability due to a thickness of several 100 µm and thermal expansion properties comparable to the Au absorber. However, the inherent toxicity of the oxides of beryllium as well as the high cost of the raw material limits its usage to high-end applications requiring sub-micrometer feature sizes [9].

2. Processing of graphite masks

A compromise, offering reduced costs and safe handling on one hand and the potential for standardization for DXRL and UDXRL applications on the other hand, is using rigid graphite as the mask membrane [2]. Therefore, it is in the mutual interest of the Louisiana-based research and development facilities of the Institute for Micromanufacturing (IfM) in Ruston and the Center of Advanced Microstructures and Devices (CAMD) in Baton Rouge to investigate the potential of graphite mask fabrication as part of their LIGA services. To evaluate the performance of graphite masks, the process scheme shown in Fig. 1 was developed and qualified.

For a direct comparison of the quality of the graphite mask with a conventional Ti mask, the latter was used to generate the primary pattern of the intermediate mask. Depending on the structural requirements, alternative processes such as optical lithography [10] or direct electron beam lithography may be used.

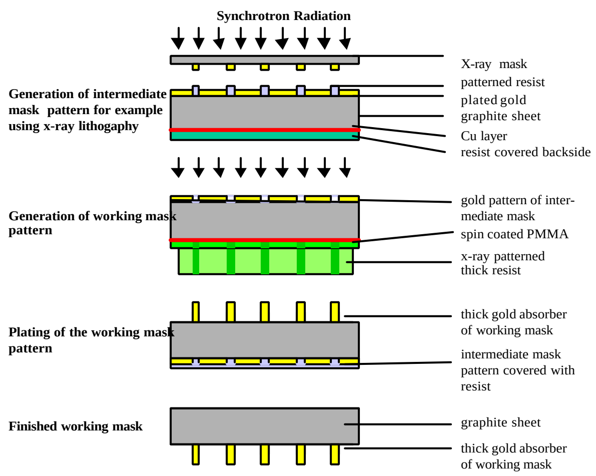

Fig. 1: Process concept for the fabrication of x-ray masks using graphite membranes.

For these experiments, off-the-shelf rigid graphite 4“ wafers 250 µm thick and of 99.95% purity were used. Thinner sheets can be used if needed [11].

The Ti mask pattern is transferred into a 15-20 µm thick spin-coated PMMA resist using soft x-rays. After development of the irradiated resist, electroplating of the Au absorber pattern up to 10 µm follows. Prior to electroplating, the backside is covered with an optical resist or tape to prevent plating. Before stripping the resist a thick PMMA sheet (up to 100 µm) is solvent bonded onto the backside of the wafer [2].

X-ray lithography is repeated to transfer the intermediate mask into the thick PMMA resist. The exposed areas are then dissolved in the GG developer at room temperature. Development is finished when the GG developer has etched through the Cu layer (approx. 100 nm thick).

Before plating up Au on the backside (the working mask side), the intermediate mask is covered with a resist again. The working mask is plated with Au absorbers up to 50 µm high. The final mask is achieved by stripping the PMMA resist and etching off the intermediate mask using aqua regia. The complete process sequence can be done using equipment installed at the IfM and at CAMD. Typical processing time is one week.

Modifications of this scheme are currently under development. For example, coating the graphite with an electron beam resist of up to 10 µm thickness. Direct write e-beam patterning of the intermediate mask will allow an even faster processing and the fabrication of smaller feature sizes. Alternatively, by omitting the intermediate mask, a thick optical resist of 30 – 50 µm can be used to directly pattern the working mask layer [12].

3. Mask qualification

3.1 Graphite transmission

Inspection with an optical microscope reveals a fairly rough surface for the graphite wafers [2]. Polishing can improve surface quality although it adds new process steps and additional cost to the mask fabrication [2]. In most cases surface anomalies on the graphite are not a problem because of the x-ray transparency of the graphite. However, defects within the bulk wafer material may result in inhomogeneous transmission properties leading to uncontrollable exposure conditions.

In order to verify the x-ray transmission, the spectromicroscopy beamline at CAMD was used for spatially resolved x-ray transmission measurements [13]. In this experiment a focused ‘white’ light x-ray beam was scanned across the wafer and data in transmission as well as fluorescence mode were recorded [14]. From the transmission data, local intensity fluctuations of up to 20% can be seen. An advanced analysis of the low transmission areas, using the fluorescence mode, showed that the stronger absorption is due to contributions from higher Z materials such as Fe, V, and Ni [15]. Simulations of this absorption effect show that the additional losses result from only a few micrometer thick residues on the surface, which are introduced by the manufacturing process. Although these impurities have no measurable effect in the lithographic process an improved surface finishing should be applied in the future to ensure more homogeneous exposure conditions.

3.2 X-ray masks on graphite

In Figs. 2 and 3 Au absorber pattern on the front (intermediate mask) and backside (working mask) of a graphite mask are shown. Both pictures demonstrate the accurate pattern transfer and the homogeneous Au plating which planarizes the rough graphite surface.

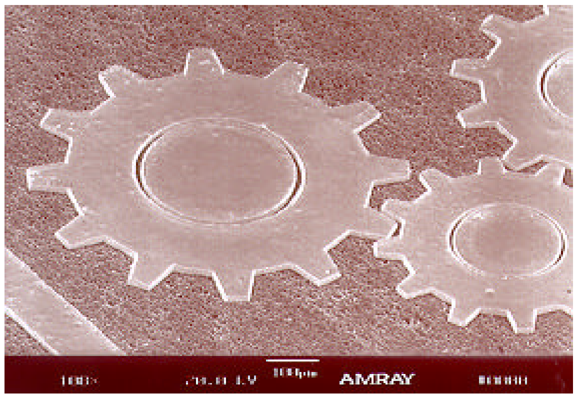

Fig 2: Intermediate mask - overview of 5 µm plated Au gear assembly on graphite

Fig 3: Working mask – 30 µm of plated Au showing the reverse image of Fig. 2.

The gold electrodeposition conditions were optimized for this work. A commercially available sulfite-based-gold electroplating solution is used for the deposition bath [16]. The parameters for gold platting are a current density of 2mA/ cm^2, a pH of 6-7, a bath temperature of 45^o C, and moderate agitation.

3.3 Working mask quality

One new and potentially critical step with respect to pattern transfer accuracy is the copying of the intermediate mask pattern through the graphite wafer. Using the reversed orientation in the x-ray exposure step the higher top dose is now deposited at the resist-substrate interface. The gaseous products formed by the radiation induced main chain scission will be trapped and may lead to some stress resulting in structural defects or lack of adhesion. However, our experience so far for resist heights up to 150 µm indicates that this causes no problems. In addition, evaluating double-sided or stacked exposures using hard x-rays [8] graphite becomes a potential candidate for a low Z substrate material.

A direct comparison of microstructures copied from the Ti 'master' mask and a graphite 'daughter' mask allows an overall measure of the process performance.

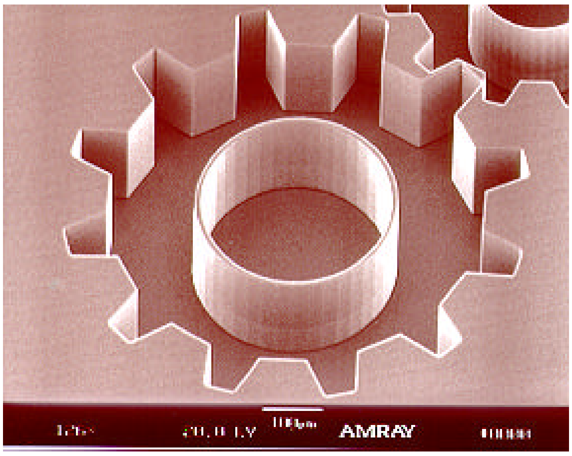

Fig. 4: SEM picture of a gear wheel structure in 150 µm thick PMMA copied from a Ti x-ray mask.

The good quality and accuracy in pattern transfer can be seen in Figs. 4 and 5. These SEM pictures show a 150 µm thick gear wheel structures in PMMA exposed from the Ti mask (Fig. 4) and from the graphite mask (Fig. 5).

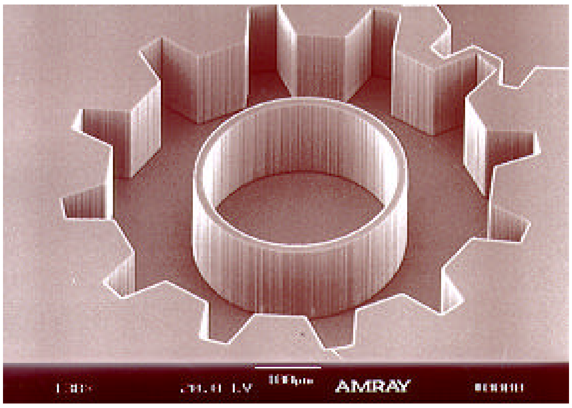

Fig. 5: SEM picture of a gear wheel structure in 150 µm thick PMMA from the graphite working mask.

A more advanced analysis of the tooth pattern geometry proved that the dimensional control is within 1 µm per sidewall and the walls produced are nearly vertical. However, when compared with the roughness of the structures achieved using the Ti mask, the sidewall roughness produced from the graphite mask is increased. The parallel vertical lines transparent from Fig. 5 are the primary source of this surface roughness.

More detailed were results obtained from an interferometric analysis using a WYKO RST profilometer [17] and are shown in Fig. 6.

From the x-direction linescans the same surface roughness (Ra ~ 20 nm) was observed as for the exposed Ti mask samples. However, in y-direction the Ra value is 200 nm indicating a higher roughness. Further investigations placed an additional graphite sheet between the Ti mask and the resist surface showed a higher sidewall roughness, too. The increase in roughness leads to the conclusion that it is caused from scattering in the graphite sheet.

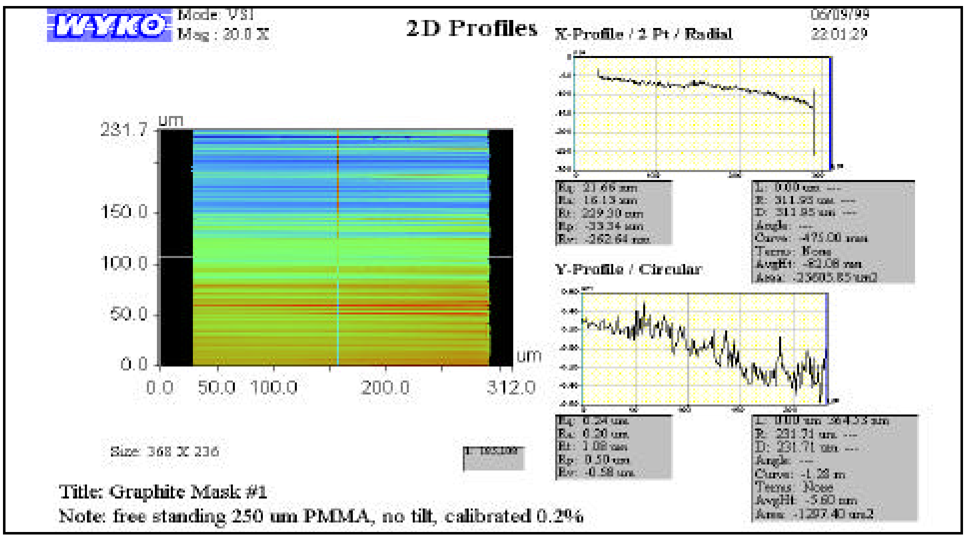

Fig. 6: WYKO RST measurement of a 250 µm thick PMMA sidewall exposed with a graphite mask.

3.4 Exposure of thick resists with a graphite mask

First exposure experiments in 1 mm thick PMMA samples were completed at the CAMD storage ring at 1.5 GeV electron energy. A typical result is shown in Fig. 7

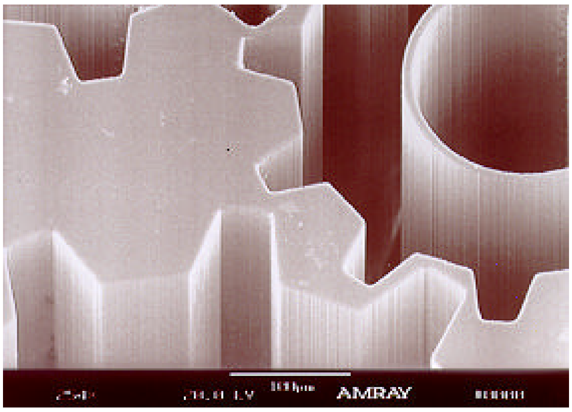

Fig 7: 1 mm thick PMMA exposed with a graphite working mask.

As evidence by the absence of cracks in the resist sidewall and minimal rounding in the top of the feature the contrast of the graphite mask is suitable for exposing ultra-high microstructures in PMMA resists.

4. Summary and Outlook

The experiments demonstrate that the mask fabrication concept using one graphite substrate as support for the intermediate and the working mask is feasible and allows the transfer of sub-micrometer features. Therefore, graphite based x-ray masks provide a cost-effective basis for bridging the transition from design concept to production allowing rapide prototyping of HAR microstructures.

In addition, the use of graphite offers some more advantages. First, graphite can be used for all three x-ray lithography ranges (XRL, DXRL, and UDXRL). Second, direct writing of small feature sizes using e-beam writing is possible. Third, the material as well as the mask fabrication process is adaptable to the specific needs of the application.

Future direction for research includes the optimization of the graphite x-ray mask performance and the development of alternative methods for the generation of the primary pattern. First results achieved using a thick optical resist to directly pattern the working mask [12] and electron beam lithography to direct write the intermediate mask pattern into 10 µm thick PMMA are encouraging.

Acknowledgments

The authors would like to thank Nick Mölders and Paul Schilling for their contributions in determining the graphite absorption from collected transmission data, using the spectromicroscopy beamline at CAMD. Yohannes Desta provided the Titanium mask that was used for this work. Work completed at the IfM was supported in part by the U S. Department of Energy under contract number DE-FG02-91CH10481.

References

[1] C. Friedrich, P. Coane, J. Göttert, N. Gopinathan; Proc. of the SPIE 22nd Annual International Symposium on Microlithography 97, SPIE Vol. 3048 (1997), pp. 193-197.

[2] P. Coane, R. Giasolli, F. DeCarlo, D. Mancini, J. Göttert; J. Vac. Sci. Technol. B16 (6), Nov/Dec 1998, pp. 3618-3624.

[3] HARMST99 Workshop Programme, Internet address www.nrlm.go.jp/harmst99/pro/harmst99programmet-English.html

[4] C. Khan Malek, K.H. Jackson, W.D. Bonivert, J. Hruby; J. Micromech. Microeng 6 (1996) 228-235 and references therein.

[5] C. Khan Malek, R. Wood, B. Dudley, Z. Ling, V. Saile; SPIE Proc. on Microlithography and Metrology in Micromachining II, Vol. 2880, (1996), pp. 160-170.

[6] W.K. Schomburg, H.J. Baving, P. Bley; Microelectronic Engineering 13, (1991), pp. 323-326.

[7] F.J. Pantenburg, S. Achenbach, M. Sesterhenn; FZKA report 6080, Forschungszentrum Karlsruhe (1998), pp. 77-82.

[8] J. Klein, H. Guckel, D.P. Siddons, E.D. Johnson; Microsystem Technologies 4 (1998) 70-73.

[9] F.J. Pantenburg, S. Achenbach, J. Mohr; J. Vac. Sci. Technol. B 16(6), Nov./Dec 1998, pp. 3547-3551.

[10] S. Ballandras, W. Daniau, S. Basrour, L. Robert, M. Rouillay, P. Blind, P. Bernede, D. Robert, S. Rocher, D. Hauden, S. Megtert, A. Labeque, L. Zewen, H. Dexpert, R. Comes, F. Rousseaux, M.F. Ravert, H. Launois; J. Micromech. Microeng. 5 (1995), pp. 203-208.

[11] Goodfellow Cambridge Limited, Cambridge, England, catalog 1995/96.

[12] C. Harris et al., “Inexpensive and Rapid X-ray Mask for LIGA”, J. Microsyst. & Tech., in press (1999).

[13] N. Mölders; Dissertation University Karlsruhe, 1999, to be published as FZKA report 6314.

[14] N. Mölders, P. J. Schilling, J.M. Schoonmaker, to be published

[15] N. Mölders, P. Schilling; private communications, detailed results to be published

[16] Technic Inc., Cranston, RI, Techni-Gold 25E, product code number 391329.

[17] S. Lippold, J. Podlesny; WYKO Surface Profilers Technical Reference Manual, WYKO, TUSCON, AZ, 1996.